A Master's Thesis

The extract of *Sageretia thea* (Osbeck) M.C.Johnst and its major active constituent inhibit melanogenesis in murine B16F10 melanoma

Gyeong-A Ko

Department of Biotechnology

Graduate School

Jeju National University

February 2016

상동 나무 추출물과 그의 활성 성분의 murine B16F10 melanoma에서의 미백활성

지도교수 김소미

고경아

이 논문을 이학 석사학위 논문으로 제출함

2016 년 2 월

고경아의 이학 석사학위 논문을 인준함

심사위원장 김 민영

위 원 김 소미

위 원 이 등순

제주대학교 대학원

2016 년 2 월

The extract of *Sageretia thea* (Osbeck) M.C.Johnst and its major active constituent inhibit melanogenesis in murine B16F10 melanoma

Gyeong-A Ko

(Supervised by Professor Somi Kim. Cho)

A thesis submitted in partial fulfillment of the requirement for the degree of Master of Biotechnology

Date Approved :

Feb. 2016

Min Young Kim

Somi Kim Cho

Dong Sun Lee

Department of Biotechnology

Graduate School

Jeju National University

February 2016

Contents

List of Tables

List of Figures

Abstract

Sageretia thea (Osbeck) M.C.Johnst. (*S. thea*), an evergreen tender shrub of the Rhamnaceae, has been used as a tisane for treating cold and a folk medicine for hepatitis as well as traditional tea materials. However, the melanogenesis affected by *S. thea* has not been investigated. The stepwise partitioned solvent fractions of the branch and fruit methanolic extracts were assessed for antimelanogenesis activities together with the identification of active compound by GC/MS analysis. Both the *S. thea* branch and fruit, the *n*-hexane fraction showed the highest inhibitory effects on melanin synthesis among the various solvent fractions. Phytol, a major constituent of *S. thea* branch, significantly reduced melanin content and cellular tyrosinase activity in a dose-dependent manner. Treatment of cells with phytol led to the downregulation of tyrosinase expression and the degradation of microphthalmia-associated transcription factor (MITF) via ERK activation, which was evidenced by recovery of melanogenesis with ERK inhibitor. In addition, phytol treatment increased ROS level, and the activation of ROS-ERK pathway by phytol induced MITF proteasomal degradation. Methyl linoleate, a major constituent of *S. thea* fruit, effectively suppressed melanin content and tyrosinase activity in B16F10 melanoma cells by decreasing phosphorylation of GSK3β which is dependent on Akt and promoting the degradation of β-catenin, thereby reducing the expression of MITF and tyrosinase family proteins. Taken together, these data indicate that *S. thea* may be a potential whitening agent in cosmetics and a therapeutic agent for treating hyperpigmentation disorders.

요 약 문

Sageretia thea (Osbeck) M.C.Johnst. (*S. thea*) 는 갈매나무과에 속하는 상록수로서, 감기치료를 위한 약탕, 간염에 대한 민간요법으로 사용되는 뿐만 아니라 차의 원료로서도 사용되지만, melanogenesis 에 대해서는 연구되어 있이 않았다. 상동 나무 잎 가지와 열매 메탄올 추출물을 각각 계통적 추출을 이용하여 분획한 후, melanogenesis activity 와 더불어 GC/MS analysis 를 통해 활성성분을 확인하였다. 상동 나무 잎 가지와 열매에서 모두 *n*-haxane 분획물이 가장 멜라닌 합성을 억제 시켰다. 상동 나무 잎가지의 major constituent 인 phytol 은 멜라닌 함량과 세포내 tyrosinase 활성을 농도의존적으로 감소시켰다. Phytol 처리에 의해 tyrosinase 발현이 감소되었고 ERK 활성화를 통한 MITF degradation 이 유도되었으며, 이는 ERK inhibitor 에 의해 다시 회복되었다. 또한 phytol 은 ROS 를 유발시켜 ROS-ERK 경로를 통한 MITF 의 proteasomal degradation 을 유도하였다. 상동 나무 열매의 major constituent 인 methyl linoleate 도 멜라닌 함량과 tyrosinase 활성을 감소시켰다. Methyl linoleate 는 Akt 의 인산화를 억제시킴으로서 GSK3β 의 인산화를 감소됨에 따라 β-catenin 의 degradation 을 유도하여 MITF 와 tyrosinase family protein 의 발현을 감소시켰다. 이 결과를 토대로 상동 나무는 화장품과 과색소침작 질병 치료를 위한 치료제로서 사용될 수 있을 것이라 사료된다.

1. Introduction

Melanin is produced by melanocytes in the basal layer of the epidermis and protects the skin from UV-induced damage, such as aging and skin cancer [1, 2]. Upon exposure to UV, keratinocytes secrete paracrine factors that promote melanin synthesis in melanocyte. Among these secreted factor, α-melanocyte-stimulating hormone (α-MSH) is a key agonist in stimulating melanogenesis [3]. Binding of α-MSH to melanocortin 1 receptor (MC1R) activates adenylyl cyclase to produce cAMP. Subsequently, cAMP activated cAMP-dependent protein kinase A (PKA) and the expression of microphthalmia-associated transcription factor (MITF), which are important for activating the genes encoding tyrosinase, tyrosinase-related protein 1 (TRP1) and TRP2 [4].

MITF is the most important factor regulating melanogenesis. MITF controls the expression of melanogenesis-related enzymes such as tyrosinase, TRP1, and TRP2, which catalyze the rate-limiting steps in melanogenesis [5]. Tyrosinase is a copper-binding glycoprotein that directly catalyzes $_{L}$-tyrosine to $_{L}$-DOPA and regulates general melanin synthesis, while TRP1 and TRP2 catalyze specific steps in melanogenesis and stabilize tyrosinase activity [5].

MITF is phosphorylated by ERK, ribosomal S6 kinase (RSK), and p38. The activation of ERK results in phosphorylation of MITF at Ser73, which induces MITF ubiquitination and degradation. RSK-1, a downstream kinase of ERK, is known to

phosphorylate MITF at Ser409, and this phosphorylation is followed by MITF degradation [6, 7].

Recently, Wnt/β-catenin signal pathway is known to play an important role in melanin synthesis. When Wnt/β-catenin signal pathway is activated, GSK3β is negatively regulated resulting in accumulation of β-catenin in cytoplasm which can be translocated into the nucleus and bind to the promoter of MITF together with LEF1 contributing to the transcription of MITF [2].

The proper amount of melanin prevents UV irradiation-induced cellular damages in skin. However, abnormal pigmentation is linked to pathophysiological conditions such as acquired hyperpigmentation, melasma, and age spots [5]. In the field of cosmetics, there are several common whitening agents, such as kojic acid and arbutin. But it has been reported that kojic acid has the ability to induce cancer and arbutin can promote melanin synthesis when its concentration is higher. As a result, it is meaningful to search for new kinds of whitening agents. Some studies have indicated that several plant components can suppress melanin synthesis and have been added to skin care product and have feasible to search for new plant components which can suppress melanin synthesis and have enormous potential [2].

Sageretia thea (Osbeck) M.C.Johnst. (*S. thea*), locally known as "Sangdong", is an evergreen tender shrub of the Rhamnaceae family native to Asia and warmer areas of North America. In Korea it grows along the southern seashore areas and traditionally the leaves have been used as tea materials [9]. It also has been used as a tisane for

treating cold and fever in Korea and a folk medicine for hepatitis in China. The leaves of *S. thea* have inhibitory activity on HIV-1 protease [11] and antioxidant activity [9, 10]. However, there have been no reports on the antimelanogensis activity of *S. thea*. Especially, there was very limited research on of *S. thea* fruit.

Thus, the objective of this study was to examine the efficacy of *S. thea* as an antimelanogenesis effect. Additionally, the major active constituents, phytol and methyl linoleate, of *S. thea* branch and fruit were further investigated the biological mechanisms underlying.

2. Materials and Methods

2.1. Reagents

Dulbecco's modified Eagle's medium (DMEM), fetal bovine serum (FBS), and 100× penicillin/streptomycin solution were purchased from Invitrogen Inc. (Grand Island, N.Y., U.S.A.). Dimethyl sulfoxide (DMSO) and 3-(4,5-dimethylthiazol-2-yl)-2,5-diphenyltetrazolium bromide (MTT) were purchased from Amresco Inc. (Solon, Ohio, U.S.A.). Phytol, methyl linoleate, α-melanocyte-stimulating hormone (α-MSH), L-DOPA, 2',7'-dichlorofluorescin diacetate (H_2DCF-DA), sodium hydroxide, mushroom tyrosinase, arbutin, kojic acid, resveratrol, MG132, and N-acetylcysteine amide (NAC) were purchased from Sigma Chemical Co. (St. Louis, Mo., U.S.A.). PD98059 was purchased from Merck Inc. (Darmstadt, Germany). MITF, tyrosinase, TRP1, TRP2, and ubiquitin antibodies were purchased from Santa Cruz Biotechnology (CA, USA). ERK, p-ERK, Akt, p-Akt, GSK3β, p-GSK3β, and actin antibodies were purchased from Cell signaling Technology (Beverly, MA, USA). β-catenin antibody was purchased from BD (Franklin Lake, USA). Silica gel (0.063–0.2 mm), (Merck, Germany), octadecyl silica gel (ODS, Lichroprep RP-18, Merck), and Sephadex LH-20 (25–100 μm), (GE Healthcare, Sweden) for gel filtration chromatography were used for column chromatography. Thin-layer chromatography (TLC) was performed on a Kiesel gel 60 F254 plate (silica gel 60, 70–230 mesh, Merck) and DC-Fertigplatten RP-18 F254S (Merck). TLC plates developed in 10% H_2SO_4 were visualized using a

Spectroline ENF 260C/F UV lamp (USA). For gas chromatography mass spectrometer (GC-MS) analysis, high-performance liquid chromatography (HPLC) grade solvents were purchased from Merck Inc. (Darmstadt, Germany). All other chemicals and reagents were of analytical grade.

2.2. Plant materials

The *S. thea* branch and fruit were collected from Swo Kwang, Jeju Island, in November 2013 and May 2014. Botanical samples were previously taxonomically identified, and voucher specimen deposited by Dr. Hui Kim at Medicinal Plants Resources, Mokpo National University, Muan-gun, Jeollanam-do, Korea.

2.3. Extraction and fractionation

The *S. thea* brunch was lyophilized for 1 day, then pulverized, and extracted with 80% methanol at room temperature with occasional sonication (maximum 60 Hz for 15 min per once) for 3 times. The extracts were filtered, concentrated with a vacuum rotary evaporator under reduced pressure at 40℃, and lyophilized to afford a crude extract. The concentrated methanol extracts were suspended in water and further fractionated by additional extraction with *n*-hexane, chloroform, ethyl acetate, and *n*-butanol in a stepwise manner. Each fractions were lyophilized to obtain the powder, and its powder was dissolved and diluted with DMSO to give final concentrations.

The *S. thea* fruit (10 kg) was extracted with 80% aqueous methanol (40 L × 3) for 24 h, giving a concentrated extract (1.6 kg). The concentrated extract was dissolved in water (8 L) and successively extracted with *n*-hexane (8 L × 3), chloroform (8 L × 3), ethyl acetate (8 L × 3), and *n*-butanol (3.6 L × 3), yielding a concentrated extract of *n*-hexane (18 g), chloroform (3.6 g), ethyl acetate (20.9 g), *n*-butanol (135 g), and water (1422.5 g) fractions. The concentrated *n*-hexane (18 g) was applied to silica gel (SiO_2) column (Φ 6 × 12 cm) chromatography (c.c.) and eluted with $CHCl_3$–MeOH (15:1, 3.2 L → 10:1, 3.2 L, → 4:1, 1.5 L → 2:1, 3 L → 2:3, 1 L → 1:2, 0.1 L). Each eluent fraction was monitored by TLC, with 18 fractions (H-1 to H-18) obtained. Fraction H-3 [1.47 g, elution volume/total volume (Ve/Vt) 0.21–0.50] was subjected to SiO_2 c.c. (Φ 3.5 × 12 cm) with elution of $CHCl_3$–MeOH (36:1), and each eluent fraction was monitored by TLC, with 14 fractions (H-3-1 to H-3-14) obtained.

2.4. Chemical composition by GC/MS

Chromatographic analysis was carried by Shimadzu gas chromatography mass spectrometry (Model QP-2010, Shimadzu Co., Kyoto, Japan) in EI (Electron Impact) mode. The ionization voltage was 70 eV and temperatures of injector and interface were 250℃ and 290℃ respectively. The capillary column used was an Rtx-5MS (30 m length, 0.25 mm i.d., and 0.25 μM, film thickness). The oven temperature programmed at 60℃ (isothermal for 2 min) was ramped to 250℃ at 5℃/min and to 310℃ at 8℃/min (isothermal for 12 min). The carrier gas Helium was used at a flow

rate of 1 mL/min with 57.4 kPa pressure, and an injector volume of 1 µL using 1:10 split ratio. Mass range was from m/z 40-500 amu. The GC-MS spectral data were compared within the WILEY9 and NIST05 libraries.

2.5. Cell culture

The murine B16F10 melanoma cell line was obtained from the Korean Cell Line Bank (Seoul, Korea). The cell lines were cultured in DMEM containing 10% (v/v) heat-inactivated FBS, 100 units/mL penicillin, and 100 µg/mL streptomycin. Cells were maintained in a humidified incubator at 37°C in 5% CO_2 atmosphere.

2.6. Cell viability

The effects of sample on the viability of B16F10 cell lines were determined by MTT colorimetric assay. The cells were seeded in 96 well culture plates. After overnight incubation, cells were treated with various concentrations of the samples for 48 h. Then, 0.1 mg MTT was added to each well, and the cells were incubated at 37℃ for 4 H. The growth medium was carefully removed and DMSO (150 µL) was added to each well to dissolve the formazan crystals formed. The intensity of produced formazan was measured immediately at 570 nm using a microplate reader. The percentage of cell viability was calculated as the percentage reduction in absorbance.

2.7. Microscopic observation of cellular morphology

The cells were seeded in 6 well plates and treated with samples. Treated cells were observed under an Olympus microscope (Olympus, Essex, UK).

2.8. Melanin content

The cells were seeded in 6 well culture plates. After overnight incubation, cells were treated with samples for 48 h. Then, the culture medium was aspirated and washed with phosphate-buffered saline. The harvested cells were centrifuged, the pellet was dissolved by 1 N sodium hydroxide (NaOH) containing 10% DMSO, and the mixture was sonicated and incubated at 80℃ for 30 min. The amount of melanin in the solution was determined by measuring the absorbance at 475 nm using the microplate reader.

2.9. Tyrosinase activity

Intracellular tyrosinase activity in B16F10 cells was examined by measuring the rate of oxidation of $_{L}$-DOPA. Cells were plated in 60 mm plates, incubated with various concentrations of samples, and treated for 48 H. The cells were lysed in lysis buffer (50 mM Tris–HCl, pH 7.5, 150 mM NaCl, 1% Nonidet P-40, 2 mM EDTA, 1 mM EGTA, 1 mM $NaVO_3$, 10 mM NaF, 1 mM DTT, 1 mM PMSF, 25 μg/mL aprotinin, and 25 μg/mL leupeptin) and incubated on ice for 30 min. The lysates were centrifuged for 30 min at 13,000 rpm and 4℃, and the supernatants were stored at -70℃ until use. The protein concentrations were measured using a BCA Protein Assay kit (Pierce, Rockford,

IL, USA). Supernatants (40 μL) and 160 μL of L-DOPA (2 mM) were placed in a 96-well transparent plate, and the absorbance at 490 nm was read every 10 min for 1 H at 37℃.

The inhibitory effect of sample on mushroom tyrosinase was evaluated by using commercial tyrosinase isolated from mushrooms. Mushroom tyrosinase activity was evaluated using following methods. An aqueous solution of mushroom tyrosinase (200 U/mL, 50 μL) was added to the wells of a 96-well transparent microplate containing 50 μL of a reaction mixture containing 2 mM L-DOPA solution and the samples (50 μL). Assay mixtures were then incubated at 37°C for 30 min, and the amount of dopachrome produced was determined spectrophotometrically at 490 nm using a microplate reader.

2.10. Western blotting

The B16F10 cells were collected and washed with cold PBS after treatment with samples. Then, the cells were lysed in lysis buffer (50 mM Tris–HCl, pH 7.5, 150 mM NaCl, 1% Nonidet P-40, 2 mM EDTA, 1 mM EGTA, 1 mM $NaVO_3$, 10 mM NaF, 1 mM DTT, 1 mM PMSF, 25 μg/mL aprotinin, and 25 μg/mL leupeptin) and incubated on ice for 30 min. The lysates were centrifuged for 30 min at 13,000 rpm and 4℃, and the supernatants were stored at –70℃ until use. The protein concentrations were measured using a BCA Protein Assay kit. Aliquots of the lysates were separated by 10–15% sodium dodecyl sulfate-polyacrylamide gel electrophoresis and transferred onto

PVDF membrane (Millipore, Billerica, MA, USA) using glycine transfer buffer (192 mM glycine, 25 mM Tris–HCl, pH 8.8, and 20% [v/v] methanol). The membranes were blocked with 5% nonfat dried milk and incubated for 5 H with primary antibodies, followed by an additional 30 min incubation with secondary antibodies in milk containing Tris-buffered saline and 0.1% Tween 20. All primary antibodies were used at a 1:1,000 dilution, and horseradish peroxidase-conjugated goat anti-rabbit or -mouse IgG were used as the secondary antibody at a 1:5,000 dilution. Then, the membranes were exposed to X-ray film, and the protein bands were detected using the BS ECL plus kit (Biosesang, Gyeonggi-do, Korea).

2.11. Immunoprecipitation

Treated cells were harvested washed with cold PBS, and lysed in 300 μL lysis buffer (20 mM Tris [pH7.5], 150 mM NaCl, 1 mM EDTA, 1 mM EGTA, 1% Triton X-100, 2.5 mM sodium pyrophosphate, 1 mM β-glycerolphosphate, 1 mM Na_3VO_4, 1 μg/mL leupeptin and 1× protein inhibitor cocktail). Lysates were incubated with primary antibodies with gentle rocking overnight at 4°C. Protein A/G agarose beads (25 μL of 50% bead slurry) were then added and samples were incubated with gentle rocking at 4℃ for 6 H, samples were then centrifuged at 14,000 rpm for 1 min at 4℃, and the pellets were resuspended with 20 μL 5× SDS sample buffer and vortexed. They were then heated at 100℃ for 5 min, separated on SDS-PAGE gels (10-12%), and transferred onto PVDF membranes using glycine transfer buffer (192 mM glycine, 25

mM Tris–HCl, pH 8.8, and 20% [v/v] methanol). Membranes were then probed by western blotting using the protocol recommended by Cell Signaling Technology.

2.12. H_2DCF-DA stain

To determine ROS level, B16F10 cells were plated in 6 well plates, treated with the samples. After treatment, the cells were incubated with 2',7'-dichlorofluorescein diacetate (DCFH-DA) for 30 min at 37℃ incubator, collected and resuspended in 0.5 mL PBS. Converting rate of the DCFH-DA to the 2',7'-dichlorofluorescein (DCF) was measured with a FACS caliber flow cytometry (Becton Dickinson, USA).

2.13. Statistical analysis

All results are expressed as averages and standard deviations using Microsoft Excel. The data were subjected to one-way analysis of variance using SPSS ver. 12.0 for Windows (SPSS, Chicago, IL, USA).

3. Results - I. Antimelanogenesis activity of phytol from *S. thea* branch.

3.1. *S. thea* branch inhibits α-MSH-induced melanogenesis.

Melanogenesis due to melanin overproduction is highly dependent on the activation of cellular tyrosinase [12]. To elucidate *S. thea* branch fractions-mediated inhibition of melanogenesis, we investigated melanin production and cellular tyrosinase activity in *S. thea* branch fractions-treated B16F10 cells. α-MSH was used as a melanogenesis inducer. As shown in Fig. 1A, *n*-hexane fraction treatment significantly decreased melanin production when compared to that in the other fractions. In addition, Fig. 1B shows that *n*-hexane fraction treatment induces inhibition of cellular tyrosinase activity in a dose-dependent manner. The chemical profile of *n*-hexane fraction detected in GC-MS analysis and quantified by their peak area (%) (Fig. 1C, Table 1). The major constituent of the *n*-hexane fraction was phytol (15.23%). According to these results, the antimelanogenesis activity of *S. thea* branch *n*-hexane fraction may results from phytol. Therefore, it was studied to evaluate antimelanogenesis effect of phytol and molecular mechanism.

Figure. 1.

A

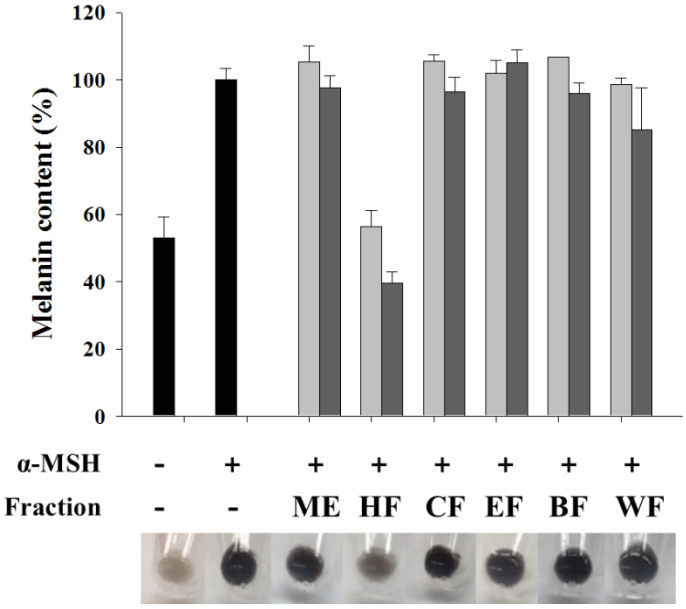

B

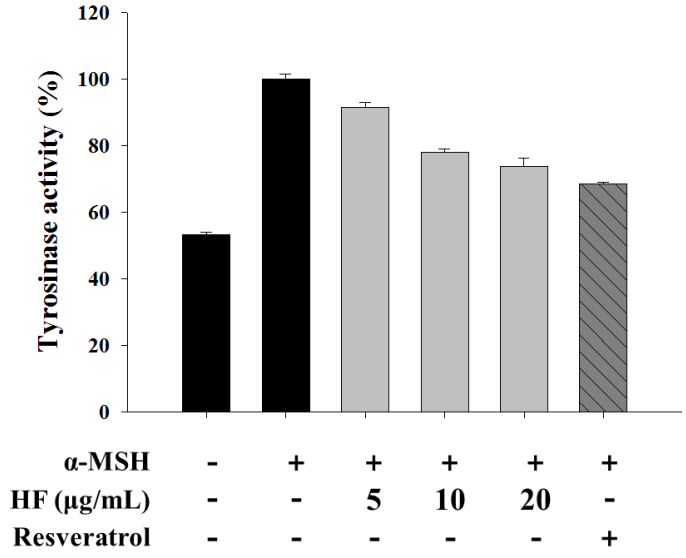

C

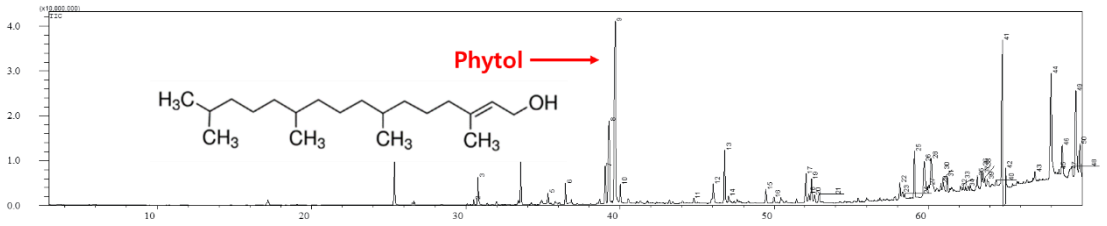

Figure. 1. *S. thea* branch inhibits α-MSH-induced melanogenesis. (A) Melanin content. (B) Intracellular tyrosinase activity. (C) GC/MS analysis. ME, methanol extract; HF, *n*-hexane fraction; CF, chloroform fraction; EF, ethyl acetate fraction; BF, *n*-butanol fraction; WF, water fraction.

Table 1. Compounds identified from the *n*-hexane fraction of *S. thea* branch by GC/MS analysis.

NO	RT (min) [1)]	Area (%)[2)]	Compound[3)]
1	25.385	3.07	Tetradecyl acrylate
2	30.790	1.59	6,10,14-Trimethyl-2-pentadecanone
3	33.561	2.88	Methyl palmitate
4	36.473	1.11	Dodecyl 2-nitrophenyl ether
5	39.039	2.15	Methyl linoleate
6	39.290	5.50	Ethyl linoleate
7	**39.701**	**15.23**	**Phytol**
8	40.021	1.08	Methyl stearate
9	46.797	3.28	δ-Undecalactone
10	52.066	1.93	2,6-dimethyl-N-(2-methyl-.alpha.-phenylbenzyl)aniline
11	52.429	1.71	1-Propene, 3-(2-cyclopentenyl)-2-methyl-1,1-diphenyl-
12	58.139	1.08	Oleamide
13	59.101	2.46	Lycopersene
14	59.732	3.91	δ-Tocopherol
15	60.943	1.01	1,2,3,5-Tetraisopropylcyclohexane
16	61.223	1.02	Solanesol
17	63.541	1.00	2-benzyloxy-2-methylhept-3-ene
18	64.818	13.69	α-Tocopherol-β-D-mannoside
19	67.906	9.52	β-sitosterol
20	68.688	2.27	Norolean-12-ene
21	69.185	1.01	Hop-22(29)-ene
22	69.572	7.66	Lupeol acetate

[1)] RT, Retention time

[2)] Area, Peak area percentage (peak area relative to the total peak area %)

[3)] Compounds tentatively identified based on parent molecular ions, retention times, retention indices and elution order, as well as the fragmented spectra compared with the literature.

3.2. Phytol inhibits α-MSH-induced melanogenesis.

Cytotoxicity of a drug is of chief importance when the drug is used either as a medicine or as a cosmetic agent [12]. Phytol could inhibit the proliferation of B16F10 cells when concentration reached 100 μM at 72 H, while it did not show obvious cytotoxicity as the cell viability was higher than 90% at 48 H (Fig. 2A). Non-toxic phytol treatment could suppress α-MSH-induced melanin production in a dose dependent manner (Fig. 2C). Moreover, the inhibitory effects of phytol were better than common whitening agents arbutin (2 mM). Meanwhile, the melanin concentration in dendrites, and the number of dendrites were decreased by phytol, the morphology restored to the control state (Fig. 2B).

Figure. 2.

A

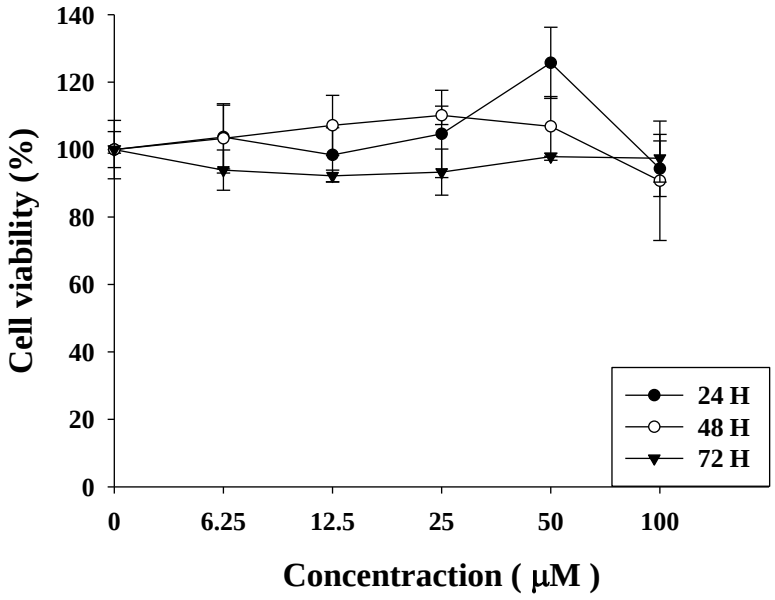

B

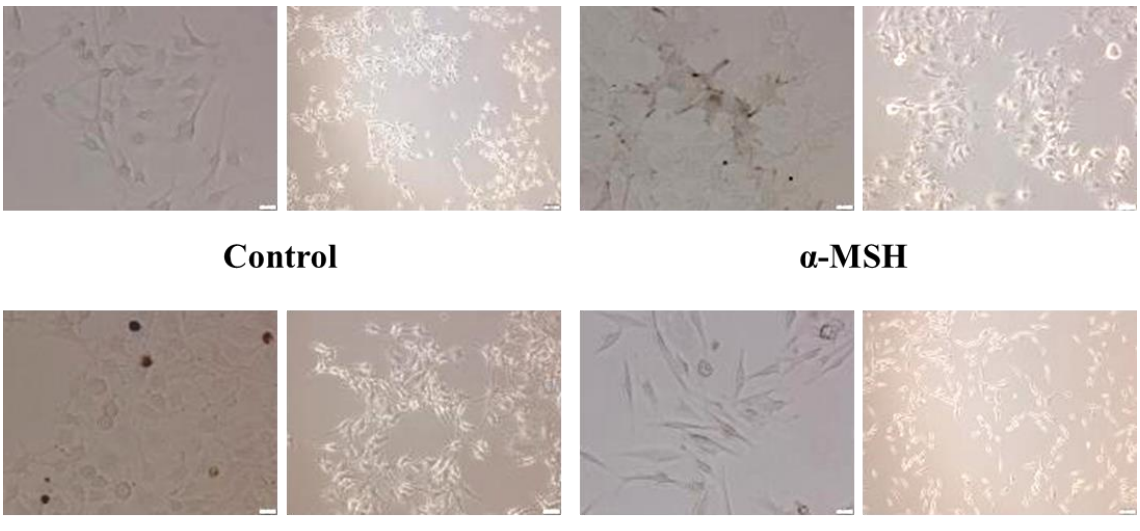

C

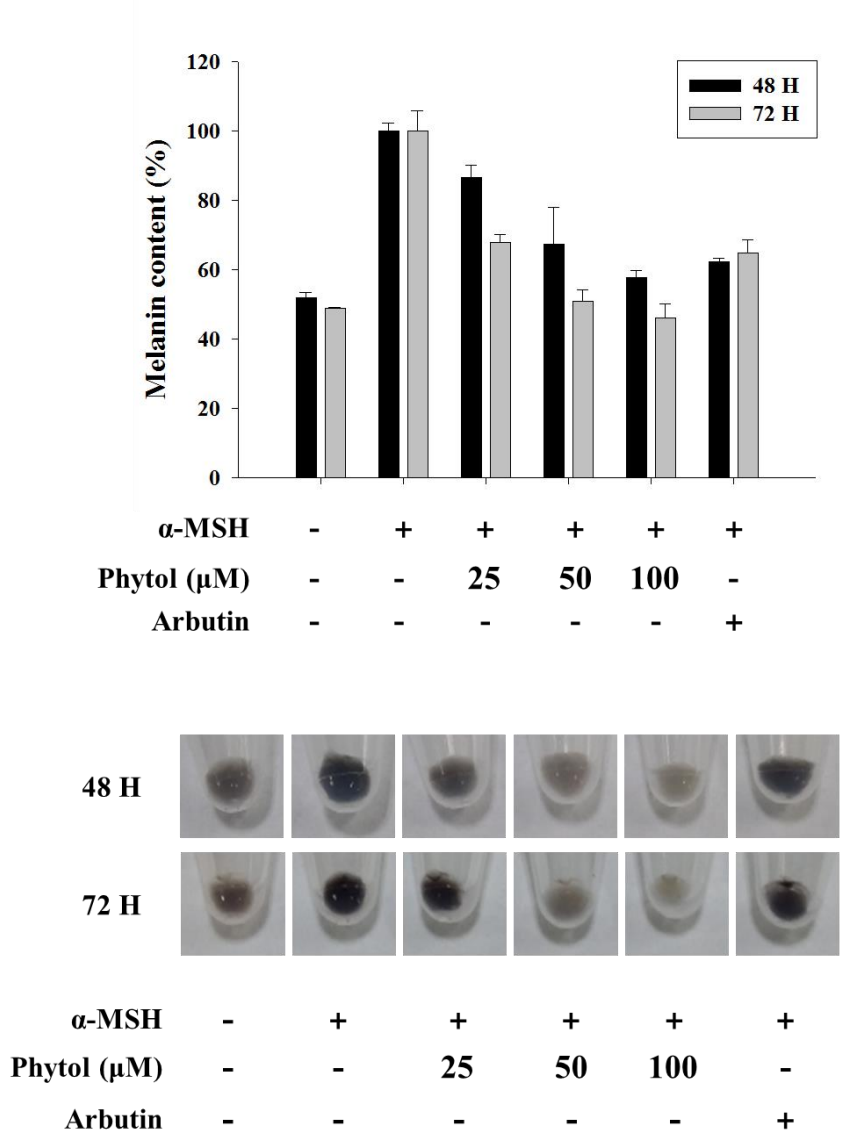

Figure. 2. Phytol inhibits α-MSH-induced melanogenesis. (A) MTT assay. (B) Cell morphology. (C) Melanin content.

3.3. Phytol inhibits tyrosinase activity and expression.

As shown in Fig. 3A, tyrosinase activity was suppressed in α-MSH-stimulated B16F10 cells with phytol treatment indicating that the decline to melanin content was also detected. Moreover, there were no obvious changes existing in activity of tyrosinase from mushroom whether treated with phytol or not (Fig. 3B). The data indicated that phytol did not directly regulate tyrosinase activity in the *in vitro* system, but did inhibit the tyrosinase expression. Therefore, we determined the levels of tyrosinase-related proteins, such as tyrosinase, TRP1, and TRP2, by western blotting after the α-MSH-stimulated B16F10 cells were treated with phytol. When measured after 48 H treatment, the levels of tyrosinase expression were repressed with increasing concentrations of phytol. However, we did not observe any significant changes in TRP1 and TRP2 protein expressions. Tyrosinase is the first enzyme in the melanin synthesis pathway, and it plays a crucial role in the regulation of melanin synthesis [1]. Although TRP1 and TRP2 did not changed, phytol inhibited melanogenesis through inhibition of tyrosinase expression.

Figure. 3.

A

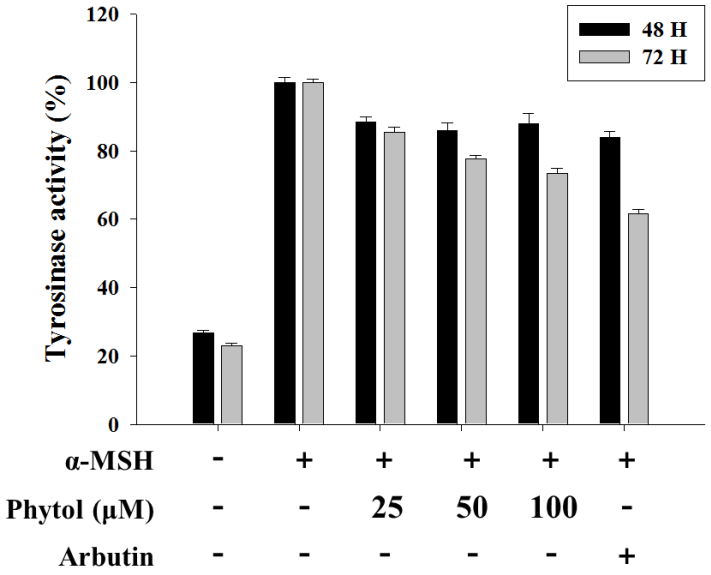

B

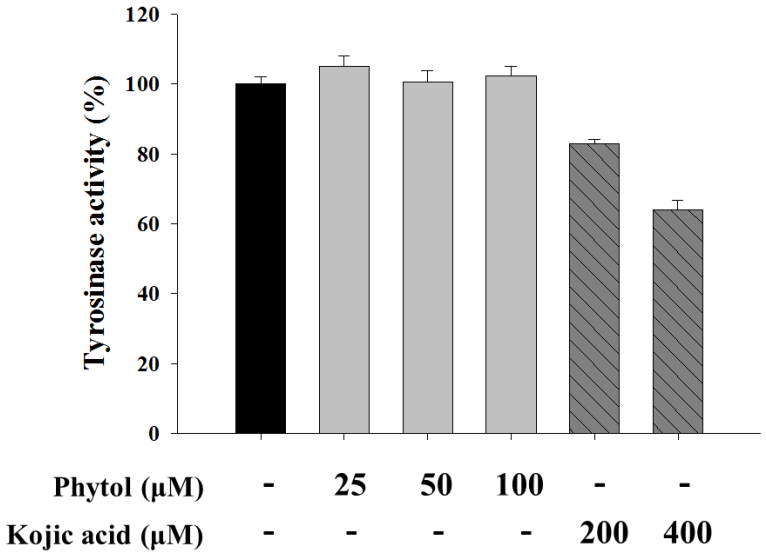

C

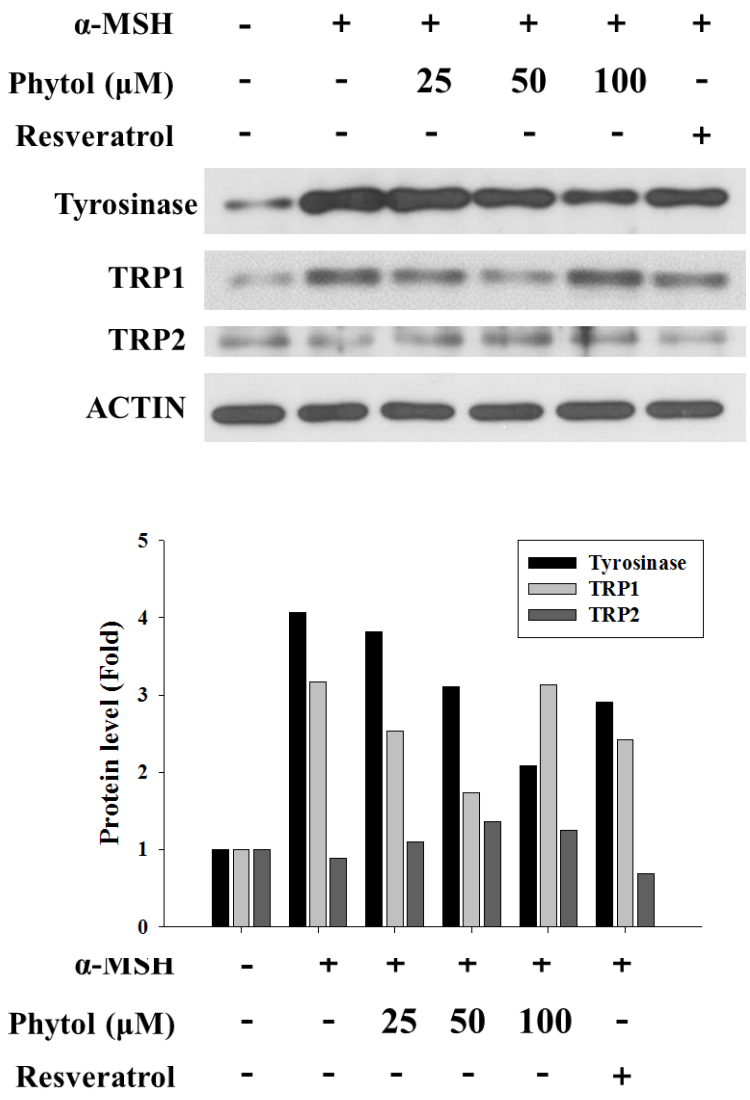

Figure. 3. Phytol inhibits tyrosinase activity and expression. (A) Intracellular tyrosinase activity. (B) Mushroom tyrosinase activity. (C) Western blot.

3.4. Phytol inhibits melanogenesis via ERK-MITF.

MITF is the common and major transcriptional regulator governing the expression of pigment enzymes, tyrosinase, TRP1, and TRP2 [8]. Many reports have demonstrated activated phosphorylation of MAPK such as ERK, Akt, and p38 to be associated with degradation of MITF, inhibition of tyrosinase synthesis and reduction of melanin production [12]. As shown in Fig. 4A, MITF expression levels reduced with phosphorylation of ERK in the presence of phytol, it was shown that the activation of the ERK pathway induces MITF degradation and that phytol plays its role by activation ERK signaling.

We determined whether ERK activation mediated the antimelanogenesis effect of phytol. PD98059, a specific inhibitor of the MEK/ERK pathway, suppressed ERK activation by phytol. ERK activation and MITF degradation by phytol were inhibited by the PD98059 treatment (Fig. 3B). Furthermore, the tyrosinase expression, melanin content, and tyrosinase activity were also restored by PD98059 treatment (Fig. 5A-C). However, there was not observed variation of melanin production and tyrosinase at a concentration of 100 μM, which may expect inhibition of melanogenesis through other signal pathway.

Figure. 4.

A

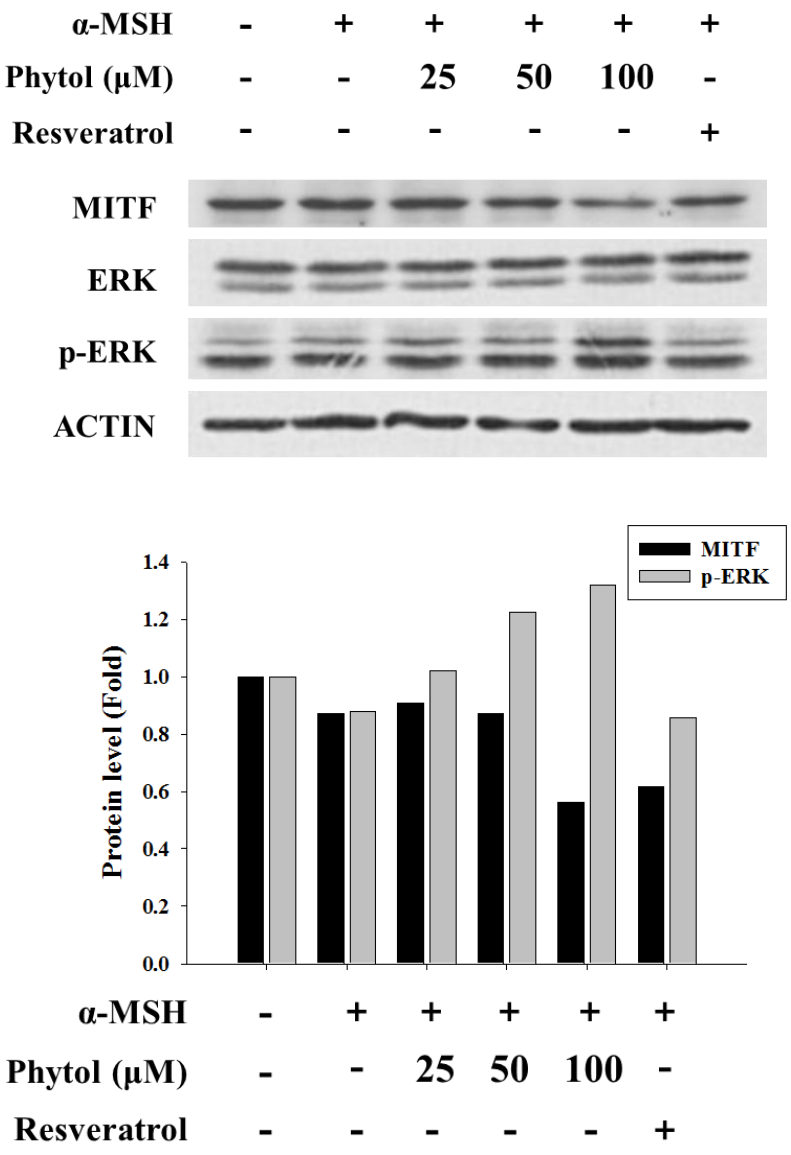

B

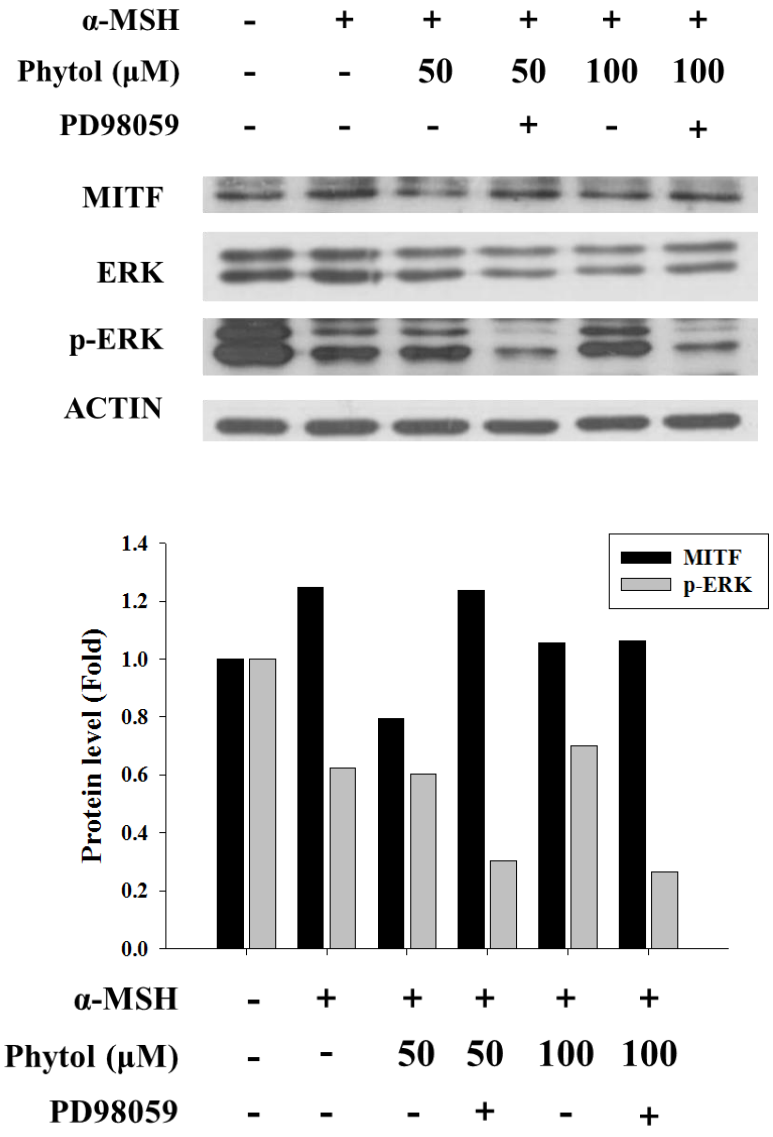

Figure. 4. Phytol decreases MITF via ERK phosphorylation. (A) Western blot. (B) Western blot with ERK inhibitor.

Figure. 5.

A

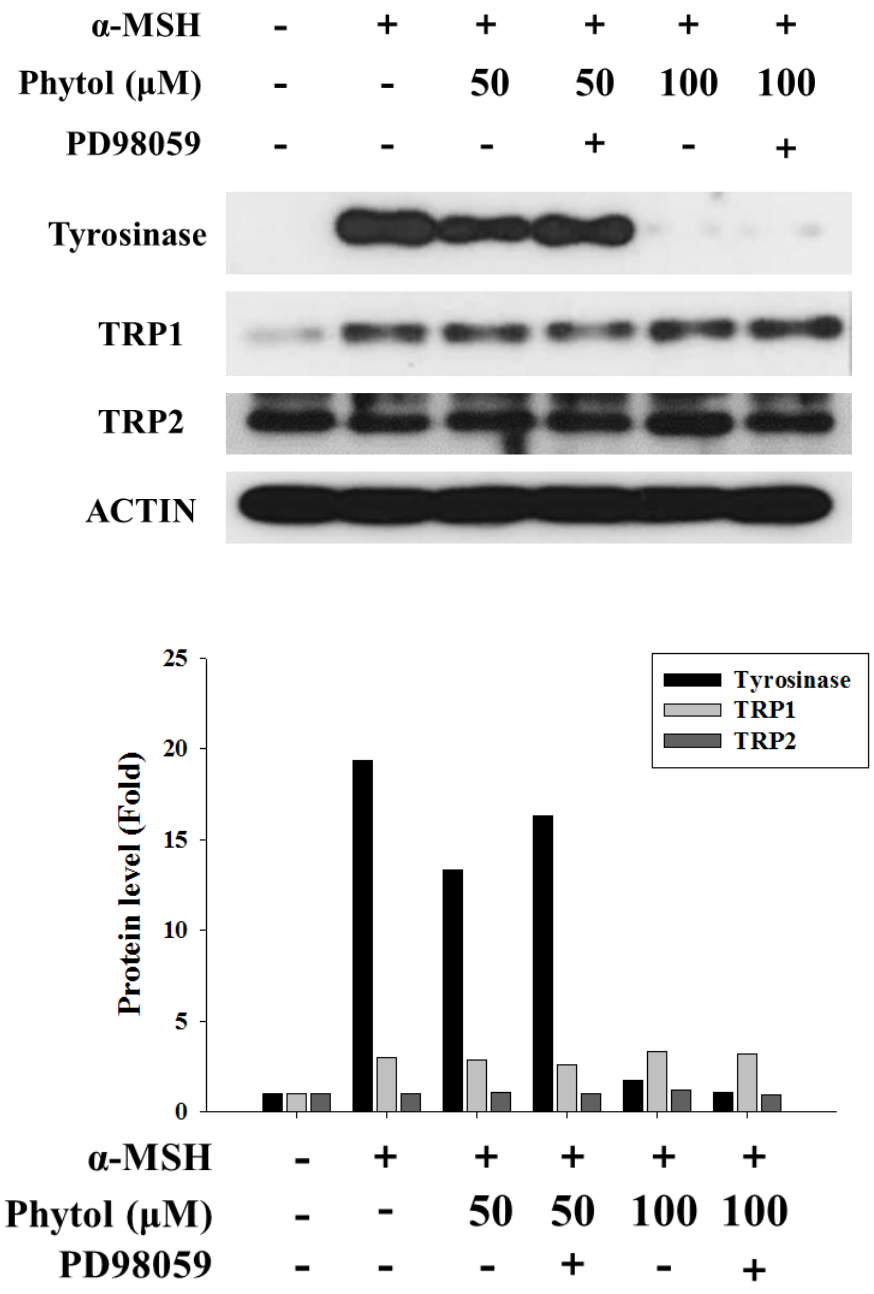

B

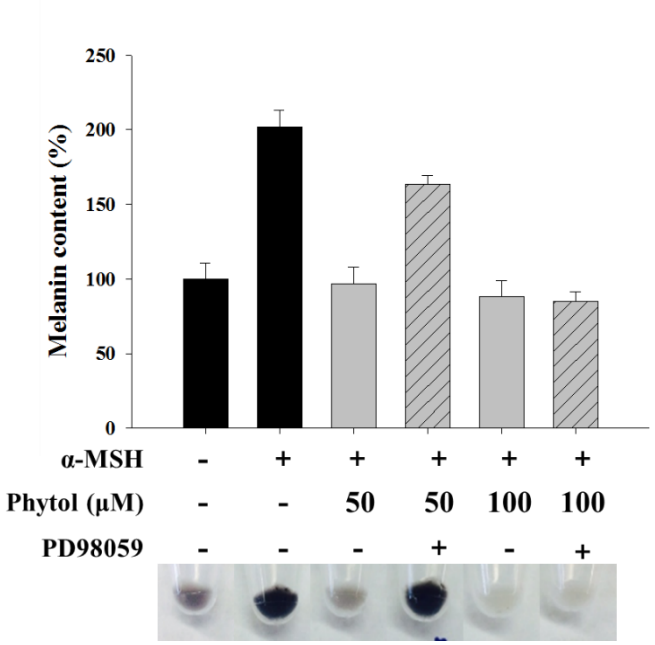

C

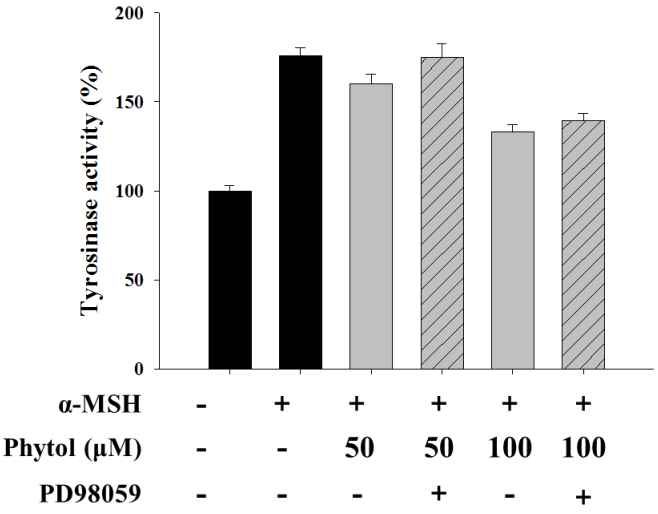

Figure. 5. Phytol inhibits melanogenesis via ERK phosphorylation. (A) Western blot. (B) Melanin content. (C) Intracellular tyrosinase activity.

3.5. Phytol induces proteasomal degradation of MITF.

To confirm that phytol-induced MITF degradation is mediated by ubiquitin-proteasome pathway, B16F10 cells were treated with MG132, a proteasome inhibitor. Treatment with a MG132 reduced the degradation of MITF (Fig. 6A). In addition, treatment with phytol in the presence of MG132 showed increase in ubiquitinated proteins compared with MG132-treated control (Fig. 6B). We then performed immunoprecipitation analysis to more critically evaluated the effects of phytol on the ubiquitination of MITF. Fig. 6C showed that ubiquitinated MITF was increased, while the MITF of whole cell lysates was decreased. These results suggested that ERK activation by phytol induces MITF ubiquitination and degradation.

Figure. 6.

A

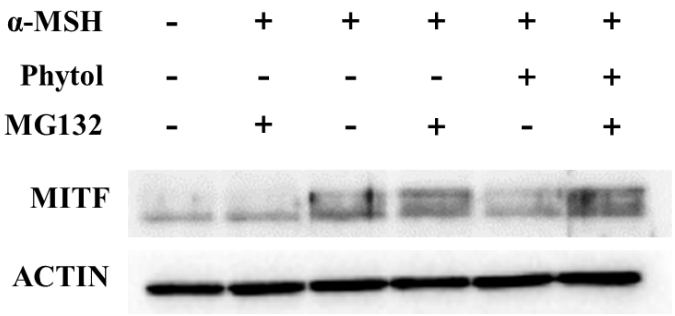

B

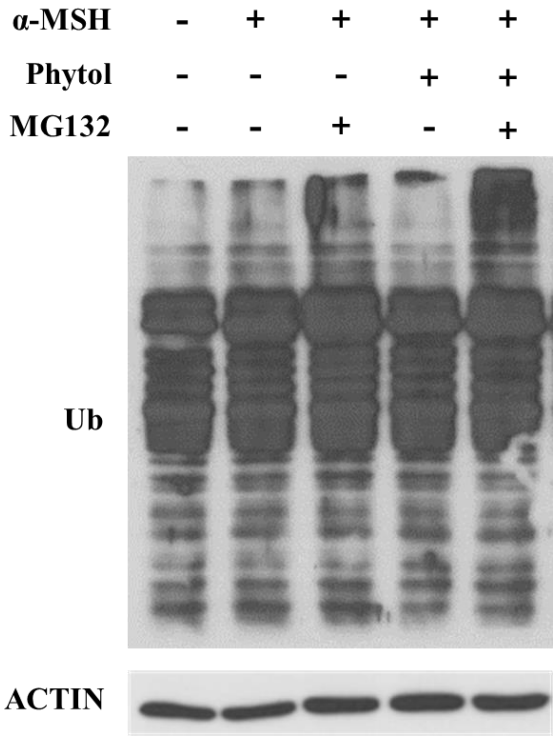

C

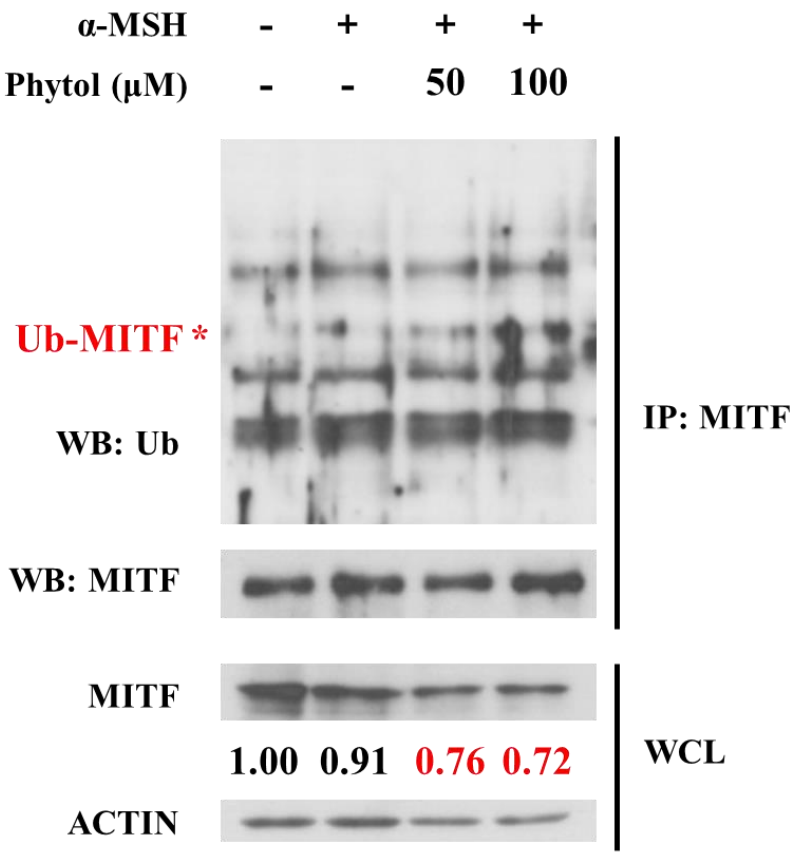

Figure. 6. Phytol induces proteasomal degradation of MITF. (A), (B) Western blot with proteasome inhibitor. (C) Immunoprecipitation assay.

3.6. Phytol-induced ROS reduces melanogenesis through ERK activation.

ROS may serve as a second messenger in signal transduction to regulate cellular processes. The MAPK signaling pathway, which is involved in antimelanogenesis, is activated by ROS stimuli [5]. Therefore, we investigated the effect of ROS on antimelanogenic activity of phytol. Treatment with phytol significantly increased ROS production on time- and dose-dependent manner at 1 to 6 H (Fig. 7A). However, the ROS levels were diminished by treatment with the ROS scavenger, NAC (Fig. 7B). To explore the molecular mechanism underlying ROS and melanogenesis, we examined the signaling pathways that are involved in the regulation of melanogenesis. The ERK phosphorylation by phytol was appreciably diminished following NAC treatment (Fig. 7C). Moreover, treatment with NAC restored the reduction of MITF expression. Taken together, these results suggested that ROS-ERK activation induced by phytol regulates melanogenesis through modulation of MITF degradation.

Figure. 7.

A

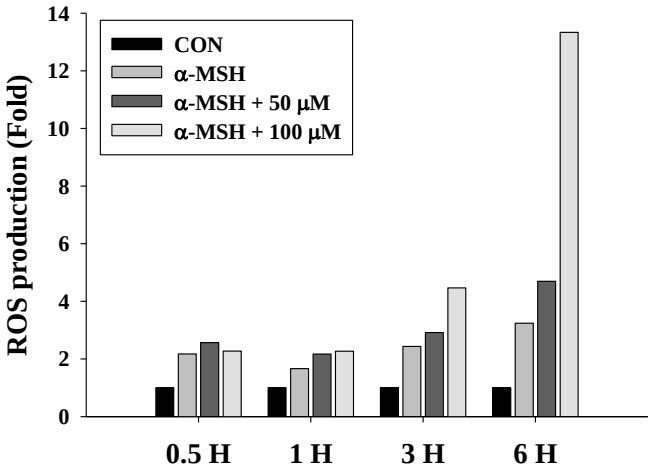

B

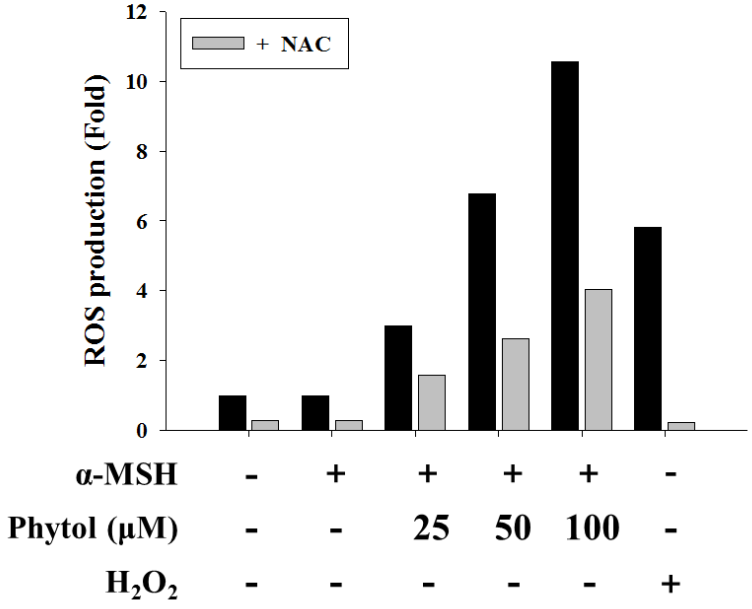

C

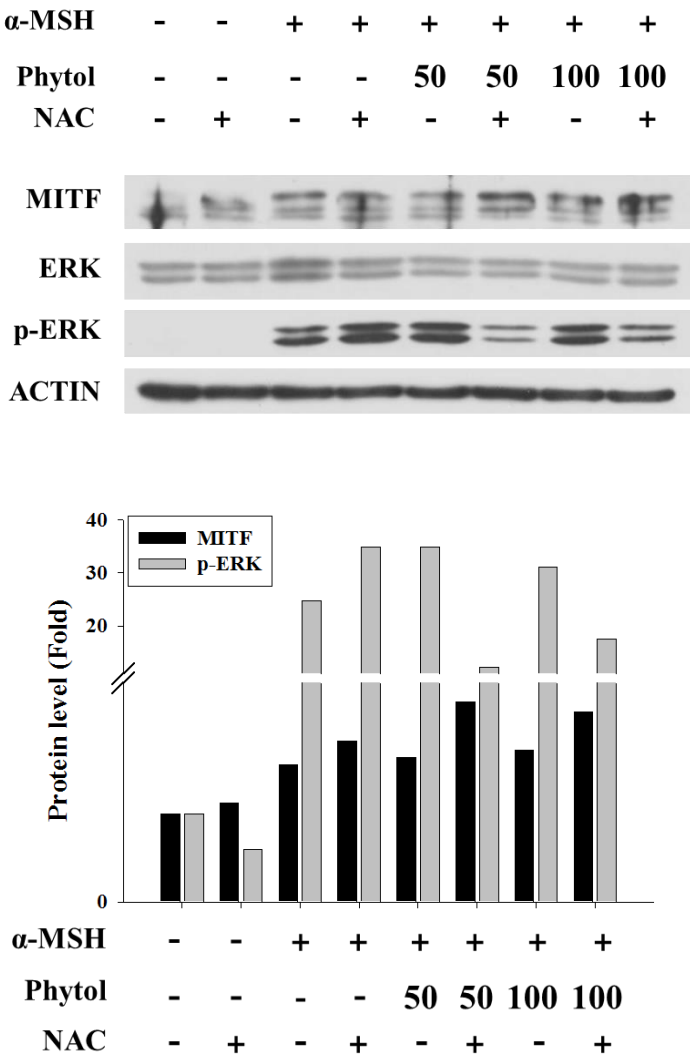

Figure. 7. Phytol-induced ROS reduces melanogenesis through ERK activation. (A) H_2DCF-DA staining for time course. (B) H_2DCF-DA staining for 6 H. (C) Western blot.

4. Results - II. Antimelanogenesis activity of methyl linoleate from *S. thea* fruit.

4.1. *S. thea* fruit inhibits α-MSH-induced melanogenesis.

The effects of *S. thea* fruit on melanogenesis were investigated in α-MSH induced B16F10 melanoma cells. Methanol, *n*-hexane, chloroform, ethyl acetate, *n*-butanol, and water fractions were prepared in a step-wise manner. The *n*-hexane fraction showed the highest the inhibitory effects on melanin synthesis among the various solvent fractions. Silica gel column chromatography and thin layer chromatography (TLC) were employed to further fractionate the *n*-hexane fraction (hexane fraction), and tested melanin synthesis of obtained fractions for enough amount. The *n*-hexane sub fractions 3 and 3-3 (H-3 and H-3-3) were found to exhibit the highest the inhibitory effects on melanin synthesis among the various sub fractions (Fig. 8).

Figure. 8.

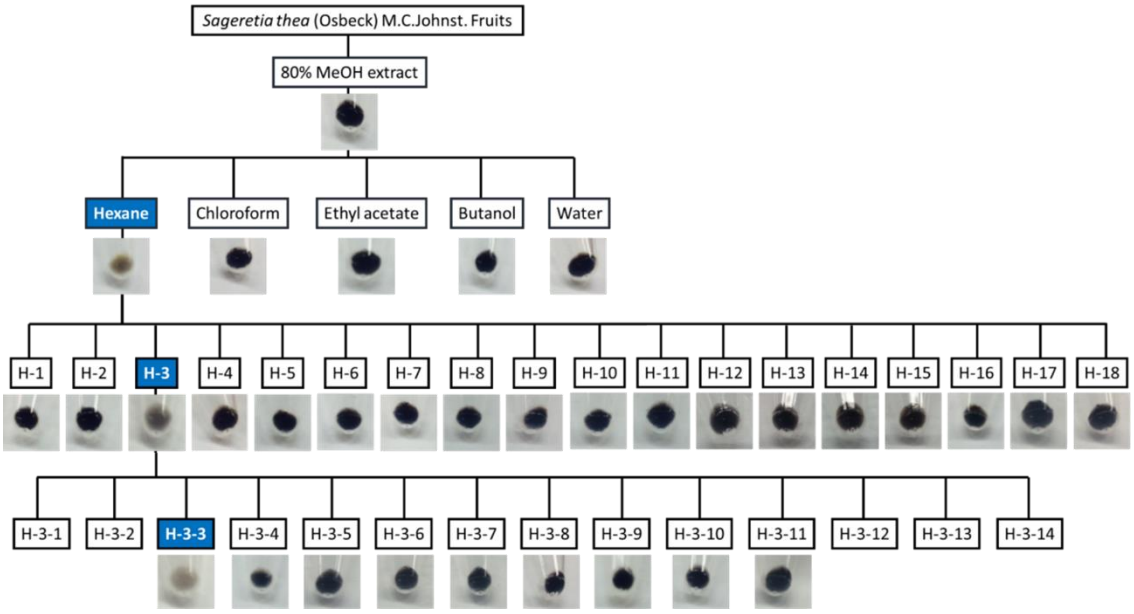

Figure. 8. *S. thea* fruit inhibits α-MSH-induced melanogenesis.

4.2. *S. thea* fruit fractions inhibit α-MSH-induced melanogenesis

We further compared antimelanogenesis activity with Hexane, H-3, and H-3-3 fractions. At the same concentrations, sub fractions more inhibit melanin production and tyrosinase activity in α-MSH-stimulated B16F10 cells (Fig. 9A, B). However, tyrosinase from mushroom activity did not suppressed in hexane fractions treatment (Fig. 9C). The hexane fractions could not change morphology of B16F10 cells apparently (Fig. 9D). The data indicated that hexane fractions probably inhibited the function of tyrosinase by decreasing tyrosinase content.

Figure. 9.

A

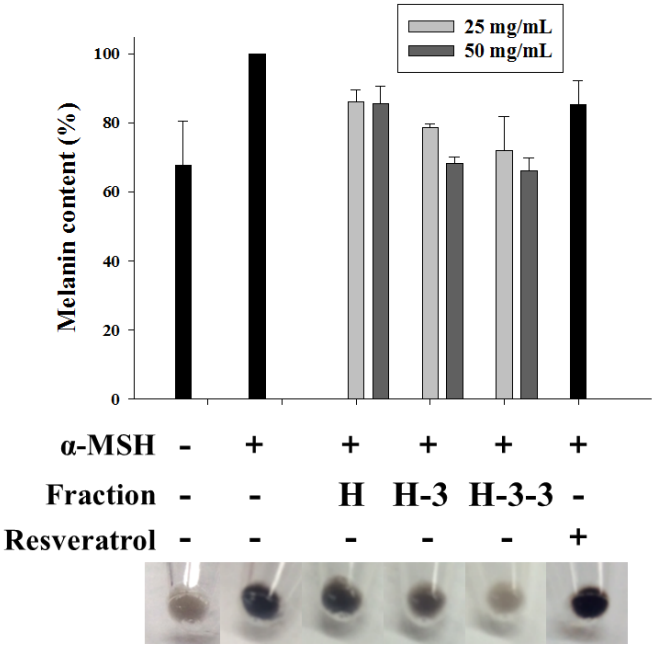

B

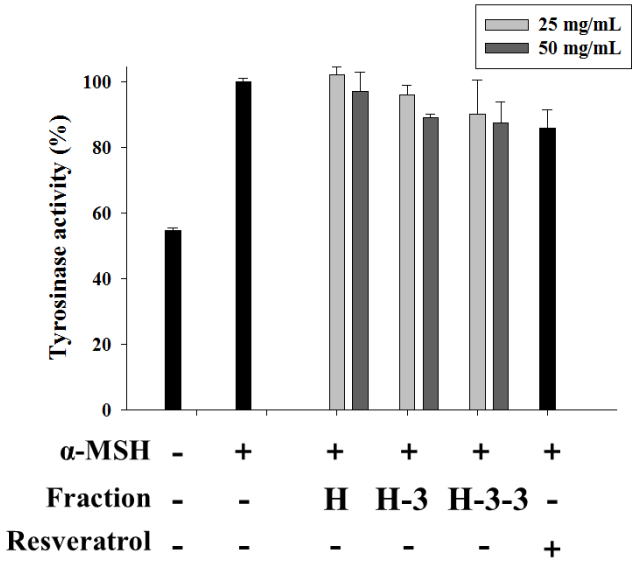

C

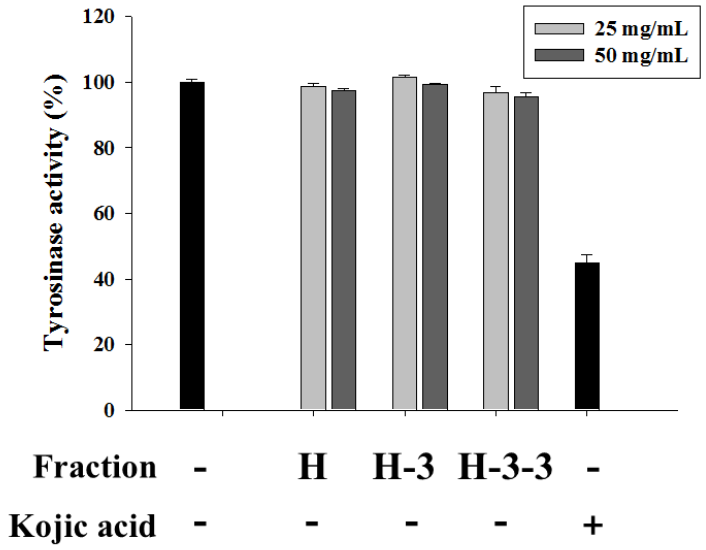

Figure. 9. *S. thea* fruit fractions inhibit α-MSH-induced melanogenesis. (A) Melanin content. (B) Intracellular tyrosinase activity. (C) Mushroom tyrosinase activity. (D) Cell morphology. H, hexane fration; H-3, H-3 fraction; H-3-3, H-3-3 fraction.

4.3. GC/MS chromatogram of *S. thea* fruit fractions.

The chemical profile of hexane and H-3-3 fractions detected in GC-MS analysis (Fig. 10, Table 2, 3). The major constituent of both the hexane and H-3-3 fractions was methyl linoleate at concentration of 0.017 and 0.197 ppm. Previously, it was reported that methyl linoleate isolated from *Oxalis triangularis* have pigment inhibition activity [14]. However, the detail mechanism of methyl linoleate was unknown. Therefore, we examined that underlying mechanism in the light of tyrosinase, TRP1 and TRP2 expression, and MITF modulation.

Figure. 10.

A

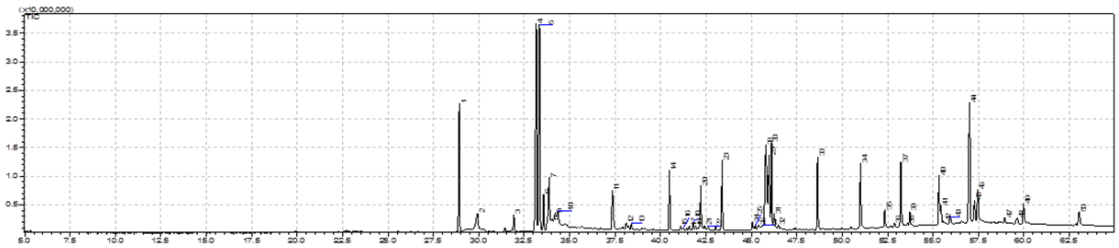

B

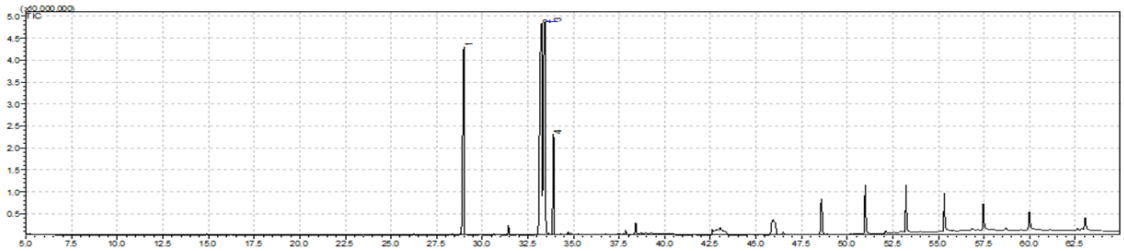

C

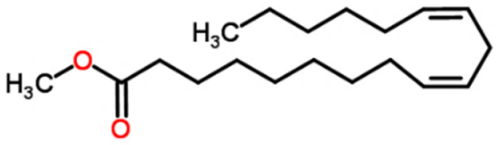

Methyl linoleate

D

Fraction	Concentration
Hexane	0.017 ppm
H-3-3	0.197 ppm

Figure. 10. GC/MS chromatogram of *S. thea* fruit fractions. (A) Hexane fraction. (B) H-3-3 fraction. (C) Methyl linoleate structure. (D) Methyl linoleate concentration of fractions.

Table 2. Compounds identified from the *n*-hexane fraction of *S. thea* fruit by GC/MS analysis.

No	RT (min) [1)]	Area (%) [2)]	Compound[3)]
1	28.922	5.42	Methyl palmitate
2	29.925	1.36	Pentadecanoic acid
3	**33.165**	**11.54**	**Methyl linoleate**
4	33.332	11.74	Methyl linolenate
5	33.558	1.43	Phytol
6	33.860	3.26	Methyl stearate
7	40.485	2.52	Octadecamethylcyclononasiloxane
8	42.214	2.46	2-Palmitoylglycerol
9	45.798	7.42	1-Monolinolein
10	45.974	4.17	Ethyl linoleate
11	55.421	1.1	Campesterol
12	57.010	7.59	β-Sitosterol
13	57.279	1.41	Fucosterol

[1)] RT, Retention time

[2)] Area, Peak area percentage (peak area relative to the total peak area %)

[3)] Compounds tentatively identified based on parent molecular ions, retention times, retention indices and elution order, as well as the fragmented spectra compared with the literature.

Table 3. Compounds identified from the H-3-3 fraction of *S. thea* fruit by GC/MS analysis.

No	RT (min) [1)]	Area (%)[2)]	Compound[3)]
1	28.994	21.64	Methyl palmitate
2	**33.257**	**37.69**	**Methyl linoleate**
3	33.421	33.85	Methyl linolenate
4	33.903	6.82	Methyl stearate

[1)] RT, Retention time

[2)] Area, Peak area percentage (peak area relative to the total peak area %)

[3)] Compounds tentatively identified based on parent molecular ions, retention times, retention indices and elution order, as well as the fragmented spectra compared with the literature.

4.4. Methyl linoleate inhibits α-MSH-induced melanogenesis.

Methyl linoleate had no effects on the growth of B16F10 cells as the cell viability was higher than 90% (Fig. 11A). As shown in Fig. 11B and C, methyl linoleate significantly decreased the melanin content without cell morphology change. In addition, Fig. 11D and E showed that methyl linoleate treatment induced inhibition of cellular tyrosinase activity in a dose-dependent manner, while did not regulate mushroom tyrosinase activity. These results indicated that methyl linoleate regulated tyrosinase family expression as the indicating hexane fractions.

Figure. 11.

A

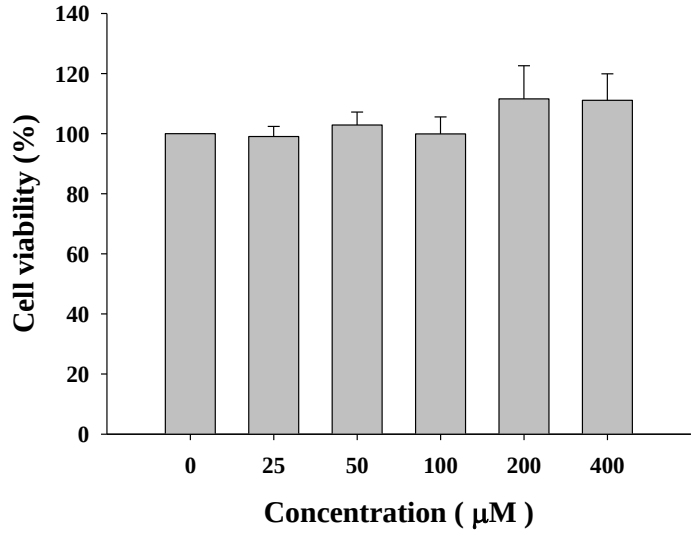

B

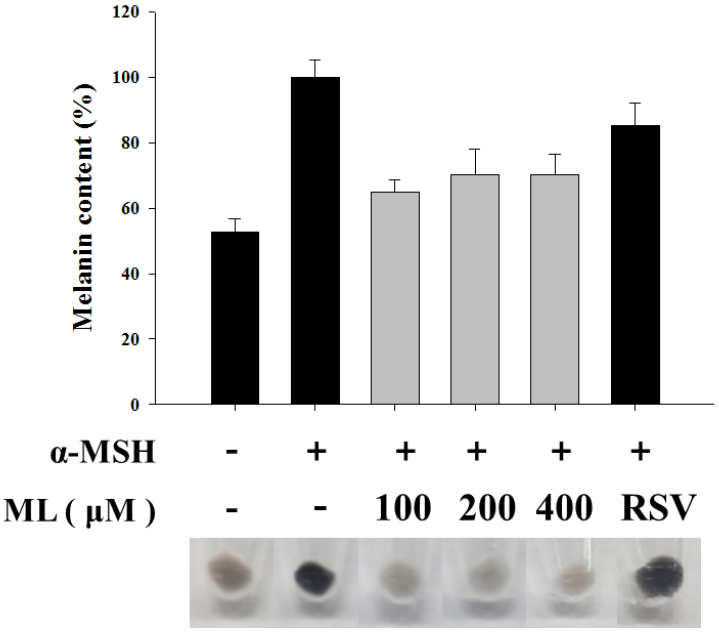

C

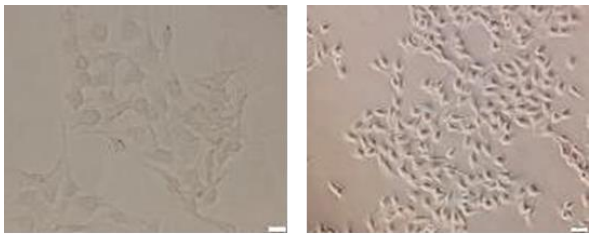

Control

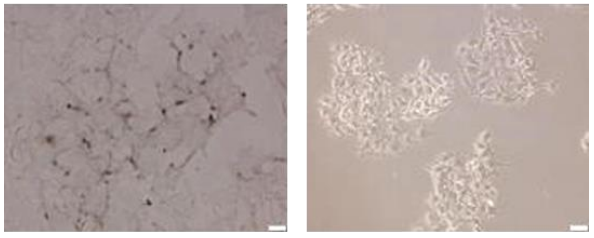

α–MSH

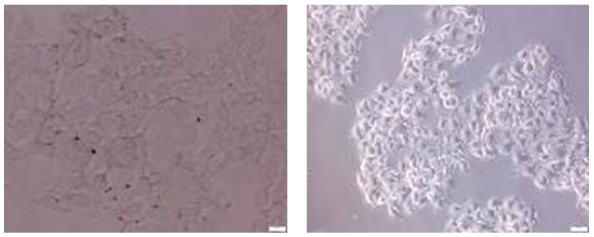

Methyl linoleate 100 μM

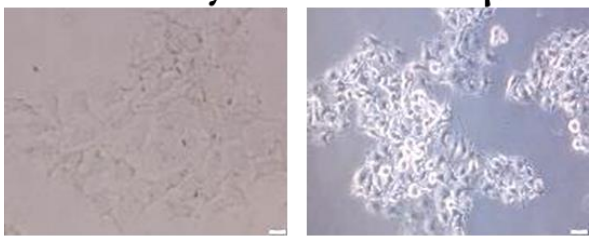

Methyl linoleate 200 μM

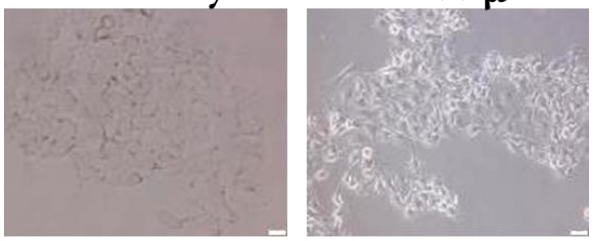

Methyl linoleate 400 μM

D

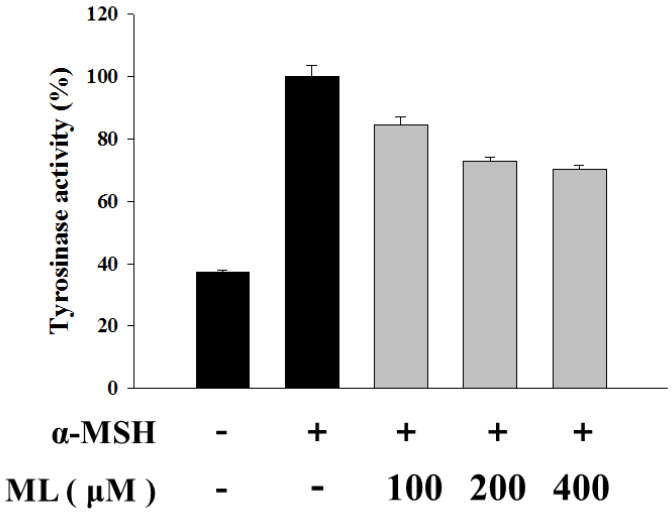

E

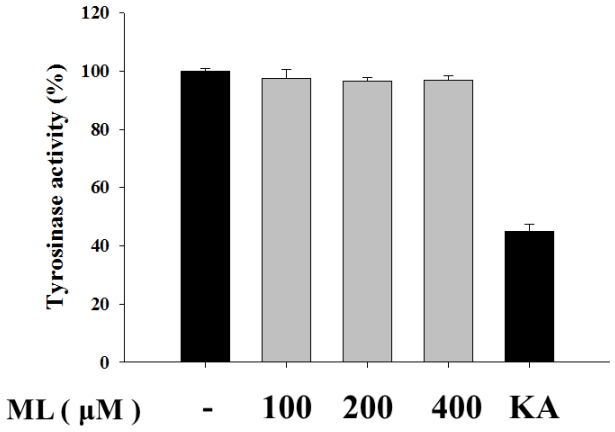

Figure. 11. Methyl linoleate inhibits α-MSH-induced melanogenesis. (A) MTT assay. (B) Melanin content. (C) Cell morphology. (D) Intracellular tyrosinase activity. (E) Mushroom tyrosinase activity. ML, methyl linoleate; RSV, resveratrol; KA, kojic acid

4.5. Hexane fraction and methyl linoleate inhibit tyrosinase expression.

To examine whether the hexane fraction and methyl linoleate regulates melanogenesis-related proteins, α-MSH-stimulated B16F10 cells were treated with hexane fraction and methyl linoleate. Protein expression levels were assessed by western blotting (Fig. 12). The hexane fraction and methyl linoleate significantly diminished tyrosinase and TRP1 expression, but slightly decreased TRP2.

Figure. 12.

A

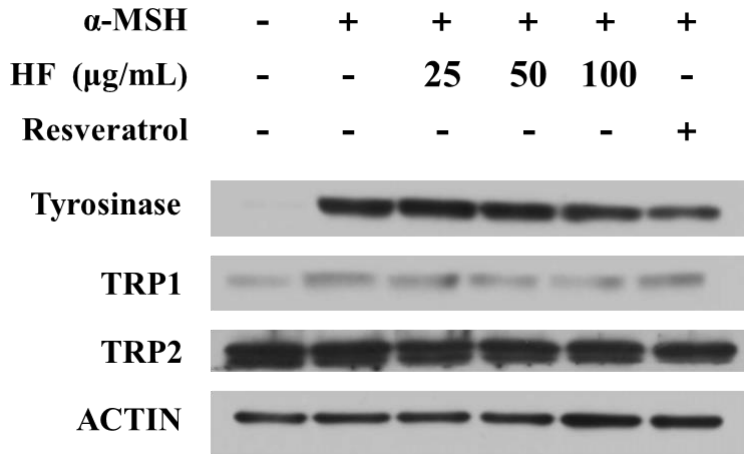

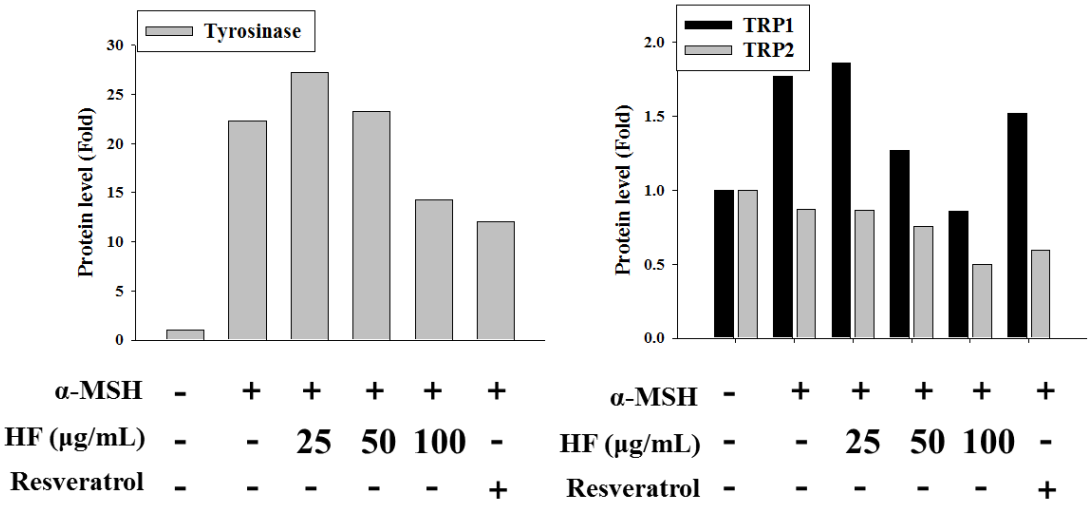

B

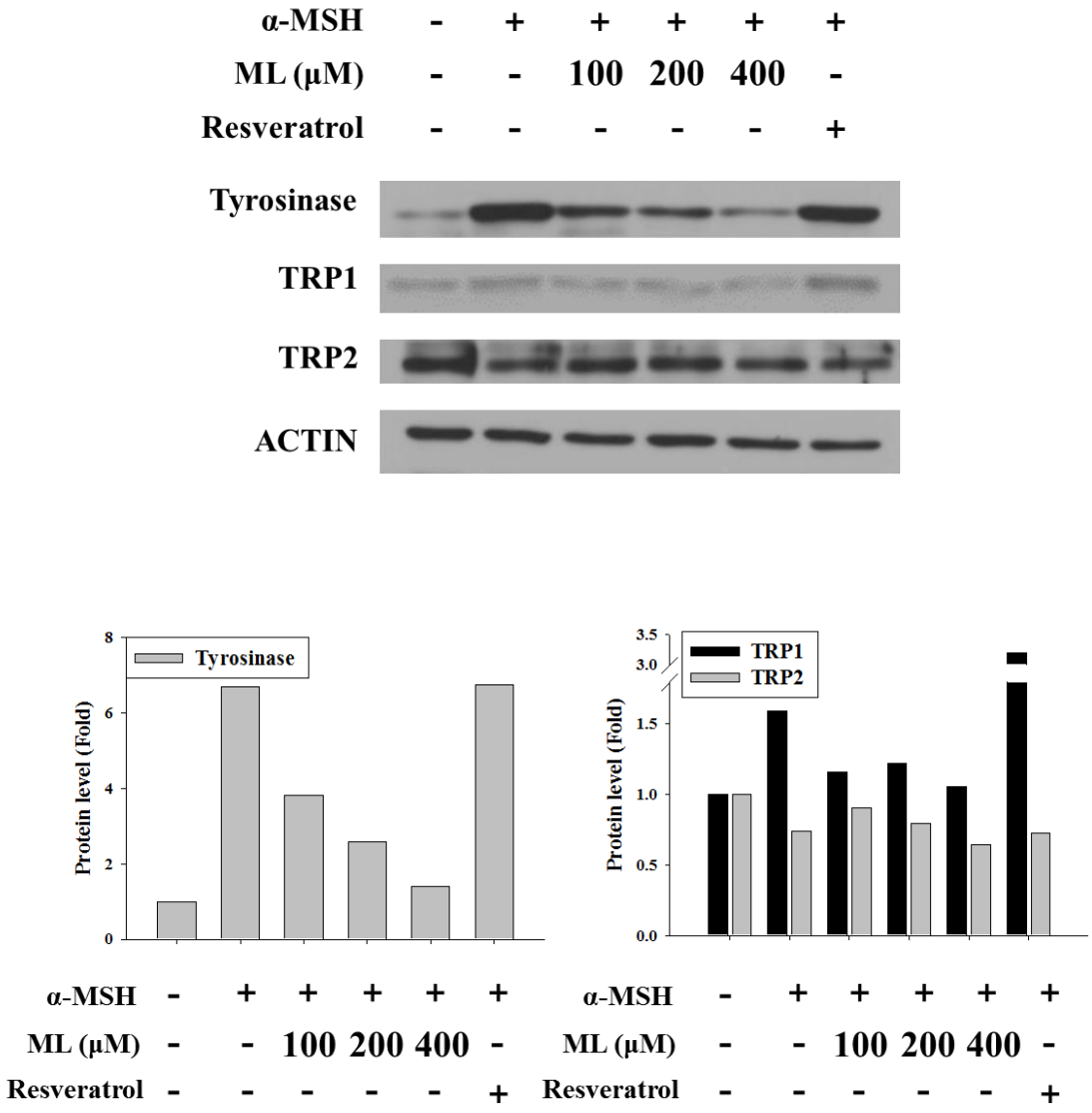

Figure. 12. Hexane fraction and Methyl linoleate inhibit tyrosinase expression.

(A) Western blot of hexane fraction. (B) Western blot of methyl linoleate. HF, hexane fraction; ML, methyl linoleate.

4.6. Hexane fraction and methyl linoleate inhibit MITF via Akt/GSK3β/β-catenin.

Previous studies have demonstrated that Wnt/β-catenin signaling controls melanocyte differentiation primarily through the direct regulation of MITF [13]. GSK3β can phosphorylate the Ser/Thr residues of β-catenin, which contributes to the degradation of β-catenin through proteasome. Therefore, β-catenin cannot bind to the promoter of MITF contributing to the transcription of MITF [2]. Fig. 13 showed that hexane fraction and methyl linoleate decreased MITF through the degradation of β-catenin. The level of phosphorylation of GSK3β also decreased in α-MSH-stimulated B16F10 cells treated with hexane fraction and methyl linoleate (Fig. 13).

It has been reported that PI3K/Akt signal pathway has a close relationship to GSK3β. Activated Akt can phosphorylated at Ser9 in GSK3β resulting in inactivating GSK3β and inhibiting the degradation of β-catenin [2]. Our data indicated that the content of p-Akt and p-GSK3β decreased by the presence of hexane fraction and methyl linoleate (Fig. 13). These results indicated that hexane fraction and methyl linoleate regulate β-catenin-dependent MITF transcription activity through Akt/GSK3β phosphorylation.

Figure. 13.

A

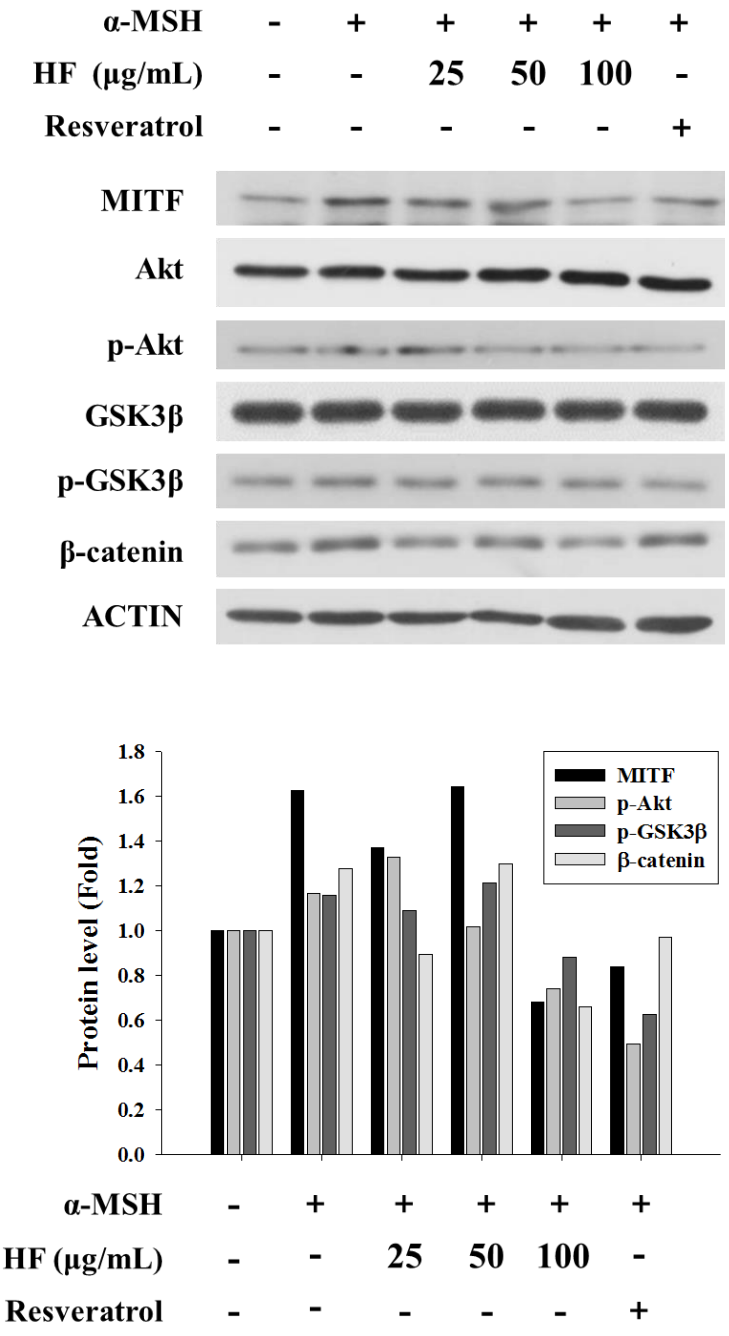

B

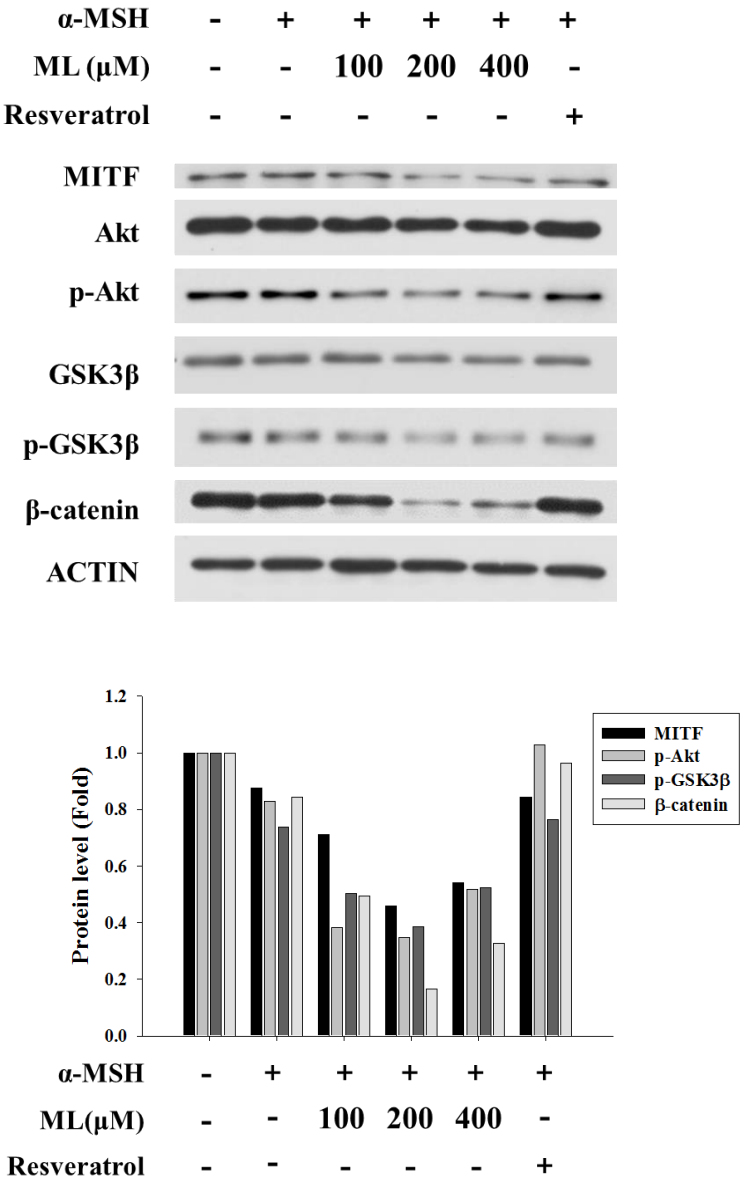

Figure. 13. Hexane fraction and Methyl linoleate inhibit MITF via Akt/GSK3β/β-catenin. (A) Western blot of hexane fraction. (B) Western blot of methyl linoleate. HF, hexane fraction; ML; methyl linoleate.

5. Conclusion

Our results indicated that phytol of *S. thea* branch and methyl linoleate of *S. thea* fruit inhibit melanin production and tyrosinase activity via downregulating MITF (Fig. 14). Phytol decreases hyperpigmentation due to MITF degradation through ROS-ERK signaling pathway. Methyl linoleate reduces the transcription activity of MITF depending on the inhibition of Akt and GSK3β phosphorylation and induction of β-catenin degradation. Consequently, the present study suggests that *S. thea* is a non-cytotoxic agent, which can be used as a skin-whitening agent both as a medicine and as a cosmetic.

Figure. 14.

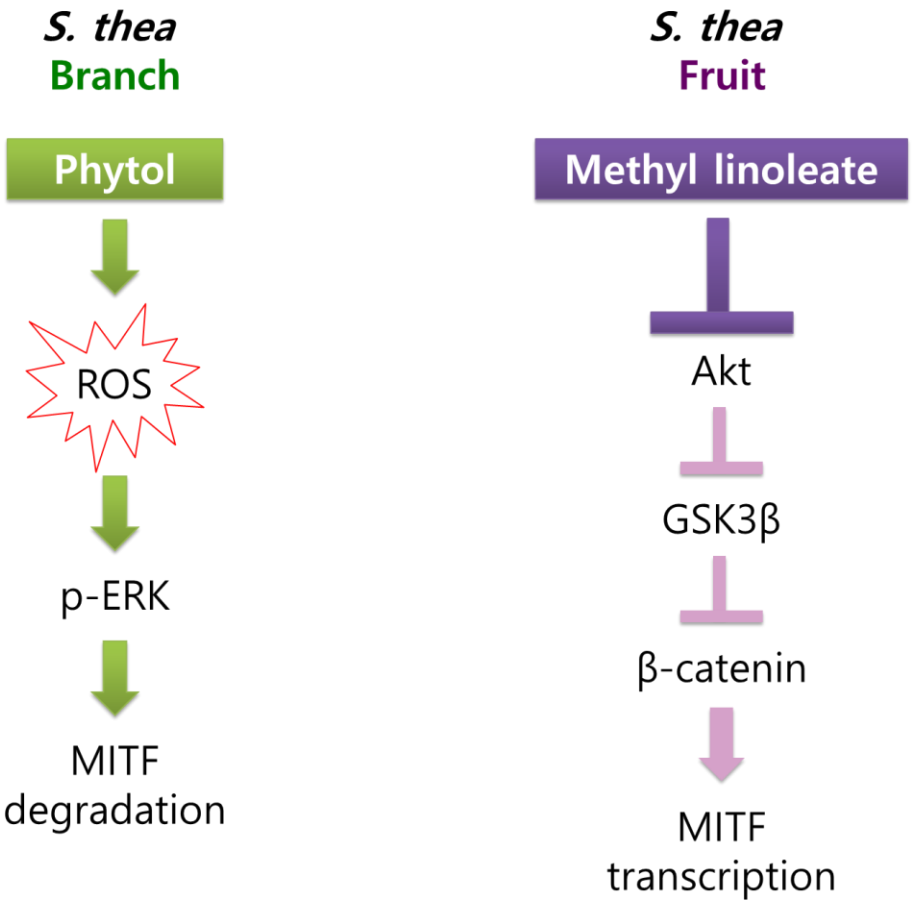

Figure. 14. Suggested mechanism of phytol and methyl linoleate-induced antimelanogenesis in murine B16F10 melanoma cell.

References

1. Lee EJ, Lee YS, Hwang S, Kim S, Hwang JS, Kim TY. *N*-(3,5-dimethylphenyl)-3-methoxybenzamide (A_3B_5) targets TRP-2 and inhibits melanogenesis and melanoma growth. J Invest Dermatol. 2011 Aug;131(8):1701-9.
2. Zhu PY, Yin WH, Wang MR, Dang YY, Ye XY. Andrographolide suppresses melanin synthesis through Akt/GSK3β/β-catenin signal pathway. J Dermatol Sci. 2015 Jul;79(1):74-83.
3. Horike N, Kumagai A, Shimono Y, Onishi T, Itoh Y, Sasaki T, Kitagawa K, Hatano O, Takagi H, Susumu T, Teraoka H, Kusano K, Nagaoka Y, Kawahara H, Takemori H. Downregulation of SIK2 expression promotes the melanogenic program in mice. Pigment Cell Melanoma Res. 2010 Dec;23(6):809-19.
4. Jung H, Chung H, Chang SE, Choi S, Han IO, Kang DH, Oh ES. Syndeca*n*-2 regulates melanin synthesis via protein kinase C βII-mediated tyrosinase activation. Pigment Cell Melanoma Res. 2014 May;27(3):387-97.
5. Kim ES, Park SJ, Goh MJ, Na YJ, Jo DS, Jo YK, Shin JH, Choi ES, Lee HK, Kim JY, Jeon HB, Kim JC, Cho DH. Mitochondrial dynamics regulate melanogenesis through proteasomal degradation of MITF via ROS-ERK activation. Pigment Cell Melanoma Res. 2014 Nov;27(6):1051-62.
6. Kim DS, Park SH, Jeong YM, Kwon SB, Miller AJ, Fisher DE, Park KC. Sphingosine-1-phosphate decreases melanin synthesis via microphthalmia-

associated transcription factor phosphorylation through the S1P3 receptor subtype. J Pharm Pharmacol. 2011 Mar;63(3):409-16.

7. Hsiao JJ, Fisher DE. The roles of microphthalmia-associated transcription factor and pigmentation in melanoma. Arch Biochem Biophys. 2014 Dec 1;563:28-34.
8. Lee CS, Park M, Han J, Lee JH, Bae IH, Choi H, Son ED, Park YH, Lim KM. Liver X receptor activation inhibits melanogenesis through the acceleration of ERK-mediated MITF degradation. J Invest Dermatol. 2013 Apr;133(4):1063-71.
9. Chung SK, Kim YC, Takaya Y, Terashima K, Niwa M. Novel flavonol gycoside, 7-O-methyl mearnsitrin, from *Sageretia theezans* and its antioxidant effect. J Agric Food Chem. 2004 Jul 28;52(15):4664-8.
10. Chung SK, Chen CYO, Blumberg JB. Flavonoid-rich fraction from Sageretia theezans leaves scavenges reactive oxygen radical species and increases the resistance of low-density lipoprotein to oxidation. J Med Food. 2009 Dec;12(6):1310-5.
11. Park JC, Hur JM, Park JG, Hatano T, Yoshida T, Miyashiro H. Min BS, Hattori M. Inhibitory effects of Korean medicinal plants and camelliatannin H from Camellia japonica on human immunodeficiency virus type 1 protease. Phytother Res. 2002 Aug;16(5):422-6.
12. Horng-Huey Ko, Yao-ChangChiang, Ming-HorngTsai, Cha*n*-JungLian, Lee-FenHsu, Shu-YuLi, Moo-ChinWang, Feng-LinYen, Chiang-WenLee. Eupafolin, a skin whitening flavono idisolated from Phylanodiflora, downregulated

melanogenesis: Role of MAPK and Akt pathways. J Ethnopharmacol. 2014;151(1):386-93.

13. Bellei B, Pitisci A, Izzo E, Picardo M. Inhibition of Melanogenesis by the Pyridinyl Imidazole Class of Compounds: Possible Involvement of the Wnt/b-Catenin Signaling Pathway. PLoS One. 2012;7(3):e33021. doi: 10.1371/journal.pone.0033021. Epub 2012 Mar 13.

14. Huh S, Kim YS, Jung E, Lim J, Jung KS, Kim MO, Lee J, Park D. Melanogenesis inhibitory effect of fatty acid alkyl esters isolated from Oxalis triangularis. Biol Pharm Bull. 2010;33(7):1242-5.

Acknowledgement

학부부터 석사과정까지 저를 도와주신 모든 분들께 감사합니다. 부족한 저를 이끌어 주신 김소미 교수님의 지도 덕분에 학위과정을 마칠 수 있었습니다. 깊은 감사를 드립니다. 바쁘신 와중에 저의 연구를 심사해 주시고 조언을 아끼지 않으신 이동선 교수님, 김민영 교수님께도 감사 드립니다. 또한 옆에서 많이 도와주신 정용오빠, 호봉오빠, 연우언니, 모아, 혜림, 소예, 지연이에게도 고맙다는 말을 전하고 싶습니다. 마지막으로 저를 믿고 지지해 주었던 가족들에게도 감사의 말씀을 전합니다.

감사합니다.